Morphology evolution via self-organization and lateral and vertical diffusion in polymer:fullerene solar cell blends

MARIANO CAMPOY-QUILES[1]*, TOBY FERENCZI[1], TIZIANO AGOSTINELLI[2], PABLO G. ETCHEGOIN[3], YOUNGKYOO KIM[1,4], THOMAS D. ANTHOPOULOS[1], PAUL N. STAVRINOU[1], DONAL D. C. BRADLEY[1]* AND JENNY NELSON[1]*

[1]Department of Physics, Blackett Laboratory, Imperial College London, Prince Consort Road, London SW7 2BW, UK
[2]Dipartimento di Elettronica e Informazione, Politecnico di Milano, Pza L. Da Vinci 32, 20133, Milano, Italy
[3]The MacDiarmid Institute for Advanced Materials and Nanotechnology, School of Chemical and Physical Sciences, Victoria University of Wellington, PO Box 600, Wellington, New Zealand
[4]Organic Nanoelectronics Laboratory, Department of Chemical Engineering, Kyungpook National University, Daegu 702-701, South Korea
*e-mail: M.Campoy@imperial.ac.uk; D.Bradley@imperial.ac.uk; Jenny.Nelson@imperial.ac.uk

Published online: 20 January 2008; doi:10.1038/nmat2102

Control of blend morphology at the microscopic scale is critical for optimizing the power conversion efficiency of plastic solar cells based on blends of conjugated polymer with fullerene derivatives. In the case of bulk heterojunctions of regioregular poly(3-hexylthiophene) (P3HT) and a soluble fullerene derivative ([6,6]-phenyl C_{61}-butyric acid methyl ester, PCBM), both blend morphology and photovoltaic device performance are influenced by various treatments, including choice of solvent, rate of drying, thermal annealing and vapour annealing. Although the protocols differ significantly, the maximum power conversion efficiency values reported for the various techniques are comparable (4–5%). In this paper, we demonstrate that these techniques all lead to a common arrangement of the components, which consists of a vertically and laterally phase-separated blend of crystalline P3HT and PCBM. We propose a morphology evolution that consists of an initial crystallization of P3HT chains, followed by diffusion of PCBM molecules to nucleation sites, at which aggregates of PCBM then grow.

In the best performing organic solar cell designs reported to date, a conjugated polymer is blended intimately with a second component, usually a fullerene, to achieve a 'bulk-heterojunction' structure. The resulting large interfacial area leads to an increase in external quantum efficiency (EQE) compared with devices fabricated with the polymer alone[1,2]. Many studies have shown that device performance is related to the morphology of the blend film, that is, to the packing of the molecules and the formation of domains of different compositions, whereas blend morphology itself depends on processing conditions (see for example ref. 3). For instance, the power conversion efficiency (PCE) of devices made from blends of poly(2-methoxy-5-(3,7-dimethyloctyloxy)-1,4-phenylenevinylene) and [6,6]-phenyl C_{61}-butyric acid methyl ester (PCBM) almost trebles on changing the solvent from which the materials are processed[4].

Recent attention has focused on blends of regioregular poly(3-hexylthiophene) (P3HT) and PCBM, the material combination that has led to the highest reported PCE values so far[5–8] (4–5%). P3HT was chosen on account of the improved spectral overlap of its absorption spectrum with the solar emission spectrum, relative to poly(*p*-phenylenevinylene)-derivative polymers. Moreover, P3HT offers the added advantage of a tendency to self-organize, which can be stimulated by increasing molecular mobility. The tendency of both P3HT and PCBM to crystallize means that the final morphology of the blend can be controlled by varying the processing conditions and/or by subsequent treatments.

A number of ways to control the blend morphology have been developed. These include both deposition and post-deposition procedures, for example appropriate solvent choice[2,4,9], slow drying of spin-coated films[8,10,11], melting of bilayers[12], thermal annealing of blends[3,13] and vapour annealing of blends[14]. These different fabrication protocols tend to promote the formation of a phase-separated morphology with crystalline P3HT and PCBM domains and in all cases lead to improved photovoltaic device performance. It is also noteworthy that the best performance characteristics for devices optimized by the different treatments are comparable.

The observed correlation between domain formation and photovoltaic device performance indicates that a certain degree of segregation of the two components is beneficial. Clearly, therefore, to further exploit and optimize the performance of organic solar cells based on polymer mixtures we need to understand the mechanism of molecular rearrangement. Yet, available data on the morphologies formed are often limited to the results of lateral microscopic imaging of the treated films. Moreover, the kinetics of the morphological changes have not previously been reported.

In this paper, we use optical techniques to probe the final morphology of P3HT:PCBM (1:1 by weight) films fabricated using four different procedures, namely fast spin coating (referred

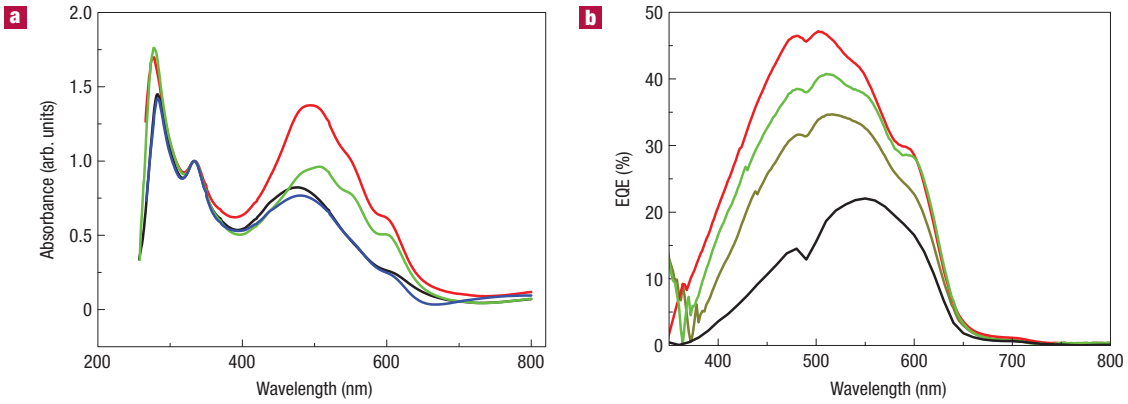

Figure 1 Absorption spectra for P3HT:PCBM films and EQE spectra for P3HT:PCBM devices. a, Absorbance spectra of P3HT:PCBM (1:1 by weight) blend films treated in the following ways: spin coated at 2,000 r.p.m. ('untreated'; black); thermally annealed at 140 °C (red); vapour annealed (green); and slow dried (spin coated at 800 r.p.m.) (blue). For the untreated and vapour- and thermally annealed samples, the films were around 150 nm thick. Slow drying results in thicker films, typically between 20 and 80% thicker depending on the specific deposition conditions. The spectra have been normalized to the isotropic PCBM peak at around 325 nm. **b**, EQE spectra (%) of indium tin oxide (ITO)/PEDOT:PSS/P3HT:PCBM (1:1)/Al devices treated in the following ways: untreated (black); vapour annealed (green); thermally annealed at 140 °C after (red) and before (olive) the deposition of the Al contact.

to as the 'untreated' case), slow drying, thermal annealing and vapour annealing. We demonstrate that a similar (optimal) morphology is attained within films prepared via the latter three protocols. Furthermore, the non-invasive nature of the selected optical techniques, including *in situ* ellipsometry and microscopy, enables us to examine in detail the mechanisms by which the morphology evolves.

The absorption spectra for films fabricated using the above methods are shown in Fig. 1a and the EQE spectra of photovoltaic devices processed by the same routes are shown in Fig. 1b. Although the devices have not been individually optimized, the thermal and vapour annealing treatments all lead to higher EQE, a more structured EQE spectrum and higher short-circuit current density (not shown) than the untreated case, in agreement with previous reports. The protocols here investigated are, therefore, of direct relevance in understanding the various treatments reported in the literature for polythiophene–fullerene solar cell optimization.

Thermal annealing and vapour annealing (as well as slow drying, not shown) induce an enhanced molecular mobility within the system, enabling spatial rearrangement of the polymer chains and fullerene molecules. P3HT chains self-assemble to form crystallites; this is reflected in both EQE (Fig. 1b) and absorption (Fig. 1a) spectra through better resolved vibronic sidebands, and particularly through the more pronounced shoulder centred at ~615 nm, which has been assigned to a highly inter-chain-delocalized excitation[15]. The intensity of this shoulder has previously been correlated with the degree of P3HT crystallinity as deduced from X-ray diffraction data[16]. For the case of thermal annealing, the formation of lamella-like crystallites with *a*-axis orientation (backbone parallel and side-chains perpendicular to the substrate) has been proposed. The latter proposal is consistent with X-ray diffraction[7,16,17], Raman spectroscopy[18], transmission electron microscopy/diffraction[17,19] and spectroscopic ellipsometry[20] data. The comparison here then implies that slow drying and vapour annealing also both result in a greater degree of P3HT crystallinity than found in untreated films.

The enhanced molecular mobility provided during thermal annealing also enables the PCBM molecules to diffuse through the film to form aggregates. The size of these domains varies from 10 to 100 nm on annealing for 5 min at 100 °C (ref. 17), up to tens of micrometres[13,18,21] on annealing for longer periods (typically >30 min) and at higher temperatures (>130 °C). The domain shape can be tuned from disc-like to needle-like by using different heating treatments and blend compositions[22], as well as by varying the degree of geometrical confinement[23]. Optical micrographs show the appearance of micrometre-sized PCBM crystalline domains on both thermal annealing and vapour annealing of our samples (Fig. 2a–c). Slow drying results in smaller PCBM domains (<200 nm) (Fig. 2d). Raman scattering enables us to confirm that these domains are indeed PCBM-rich regions (Fig. 2e,f), in full agreement with previously reported atomic force microscopy (AFM)[13], X-ray[17], transmission electron microscopy[17] and selected-area electron diffraction[21,22] data.

In order to explore the mechanisms that govern the diffusion and self-assembly processes in these systems, we have used variable-angle spectroscopic ellipsometry (VASE) to characterize films exposed to each of the treatments outlined above. VASE is a non-invasive optical probe that monitors changes in the polarization state of light on reflection from a sample[24]. It is a well-established technique for retrieval of the optical constants of thin films[24], as well as concentration–depth profiles of composite films[24–26]. The experimental data are fitted using a mathematical representation of the sample, and the quality of the fit indicates the suitability of the chosen model (see the Methods section and Supplementary Information). The model that best represents the experimental data for all of the samples we have studied consists of two layers: a blend of P3HT and PCBM whose relative concentrations vary with depth, underneath a mixed PCBM–air layer. The top layer accounts for the PCBM crystalline domains that are observed to protrude from the film[18,22]. A schematic structure is shown in Fig. 3e. According to the model fits to the data, the reference (untreated) film spin coated on fused silica comprises a composition that varies from PCBM rich close to the substrate to P3HT rich near the free (air) surface (Fig. 3a). Vertical segregation in P3HT:PCBM blends has been suggested previously[9,27,28]. Furthermore, vertical phase-separation effects have previously been observed in films of P3HT blended with isotactic semicrystalline polystyrene[29], blends of two polyfluorene copolymers[30] and blends of polyfluorene and PCBM[31,32], and have been attributed to differences in the solubilities/surface energies

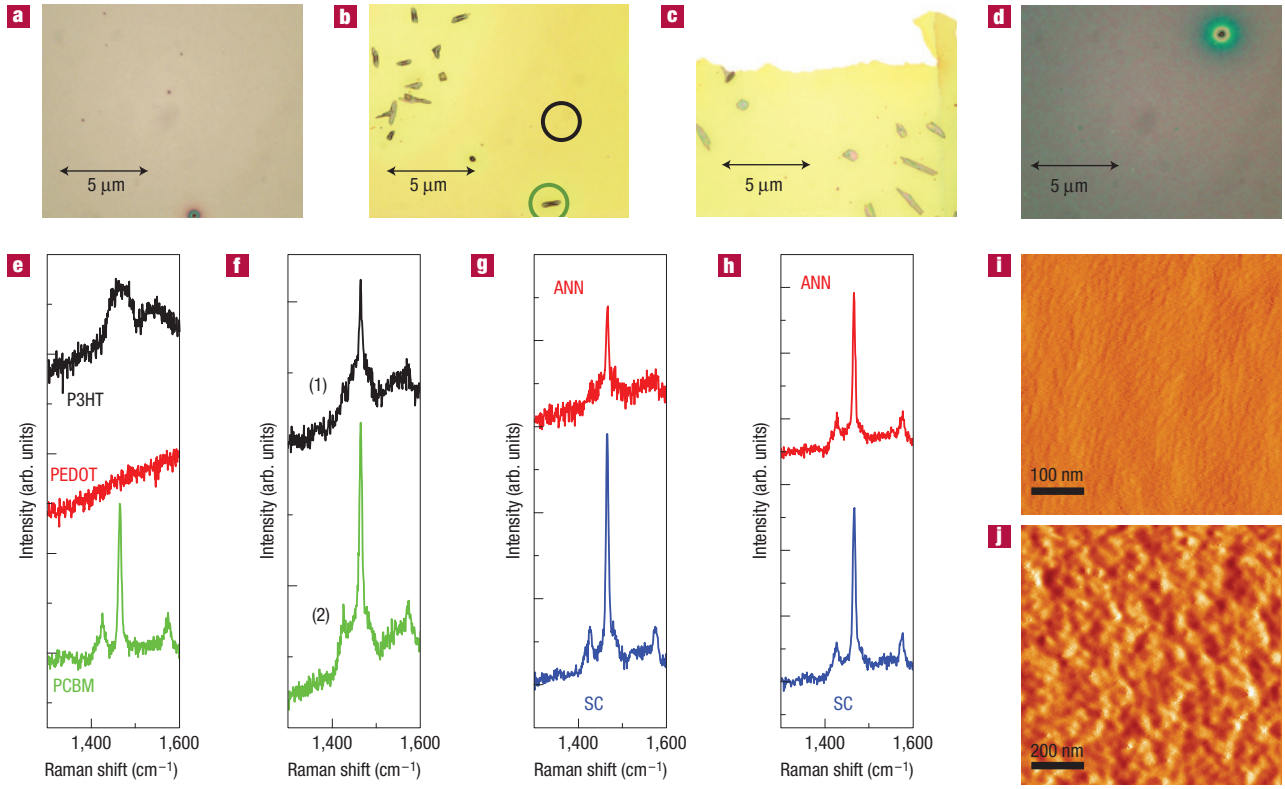

Figure 2 Lateral segregation in P3HT:PCBM films as observed by optical microscopy, Raman spectroscopy and atomic force microscopy. a–d, Optical microscope images for blend films: **a**, untreated (that is, fast spin coated), **b**, thermally annealed, **c**, vapour annealed, and **d**, slow dried. Inhomogeneities produced by impurities such as that in **d** (upper right corner of image) can often be seen in spin-coated P3HT:PCBM films. **e–h**, Raman spectra recorded using $\lambda_{ex} = 325$ nm excitation: **e**, for a spin-coated PCBM film (green line), a spin-coated PEDOT:PSS film (red) and a spin-coated P3HT film (black); **f**, for a thermally annealed P3HT:PCBM blend film (1:1) sampled at two points: (1) at a uniform region such as that encircled by the black line in **b** and (2) at a point containing a PCBM crystallite such as that encircled by the green line in **b**; **g**, for a uniform region in a blend film on fused silica before (blue) and after (red) thermal annealing; **h**, for a blend film spin coated on top of PEDOT:PSS before (blue) and after (red) thermal annealing. **i**,**j**, AFM images for a P3HT:PCBM (1:1) blend film before (**i**) and after (**j**) thermal annealing.

of the components[32] and/or the dynamics of the spin-casting process[33]. Segregation of the electron-donor material towards the anode interface and the electron-acceptor material towards the cathode interface is expected, from consideration of the effect of composition on electrode selectivity, to be beneficial for solar cell performance. Indeed, vertical composition gradients with this specific directionality have been shown to benefit solar cell performance in the case of both polymer–polymer blend devices[30,34] and vacuum-deposited molecular solar cells[35,36]. Henceforth we define a composition gradient in this sense (that is, with increasing acceptor concentration closer to the cathode) as positive. On thermal annealing, PCBM molecules diffuse out of the upper part of the blend film towards the nanoscopic PCBM domains that are already present both in the lower regions of the spin-coated film and near the air surface. This results in the formation of larger aggregates and further depletes the PCBM content within the upper, subsurface, part of the blend layer. This morphology evolution is seen in the ellipsometry results as an increase in the concentration (or thickness) of the PCBM–air surface layer, in agreement with increases in surface roughness deduced from AFM (Fig. 2i,j) and reported transmission electron microscopy images[7,17], and a more negative concentration gradient within the blend layer (Fig. 3a,f). If repeated in a device with the usual architecture, where the bottom electrode acts as anode, such a profile would reduce electrode selectivity. The proposed PCBM depletion is consistent with the observed decrease, on annealing, in PCBM Raman signal within PCBM crystallite-free regions (Fig. 2g). The growth of PCBM crystallites was monitored optically by imaging the surface of a blend film during continuous heating. Figure 4a–d shows optical micrographs of the same ($\sim 300 \times 220\,\mu m^2$) region of a PCBM:P3HT blend film at increasing temperatures (70, 160, 184 and 250 °C, ramp rate = 10 °C min^{-1}). The visibility of crystallites is limited by the $\sim 1\,\mu$m resolution of our long-focal-length system. Comparison of the 160 and 250 °C images shows a one-to-one correspondence in crystallite locations with a roughly uniform growth in crystallite size, strongly suggesting that there is an initial nucleation followed by steady growth. Higher-resolution investigations would clearly be of interest in this regard. Figure 4d (250 °C image) also shows that the regions around the crystallites become depleted of PCBM, in agreement with our Raman measurements, and with recently reported scanning near-field optical microscopy studies[19]. In particular, there is a lighter colouration evident within a halo-like region around each of the crystallites.

We next analyse the morphology changes induced by slow drying and vapour annealing. Figure 3b shows how the PCBM concentration profile changes as the spin-coating speed (and hence the rate of drying) is reduced. Slow drying has a qualitatively similar effect to thermal annealing: the composition gradient becomes more pronounced and the surface-segregated PCBM concentration

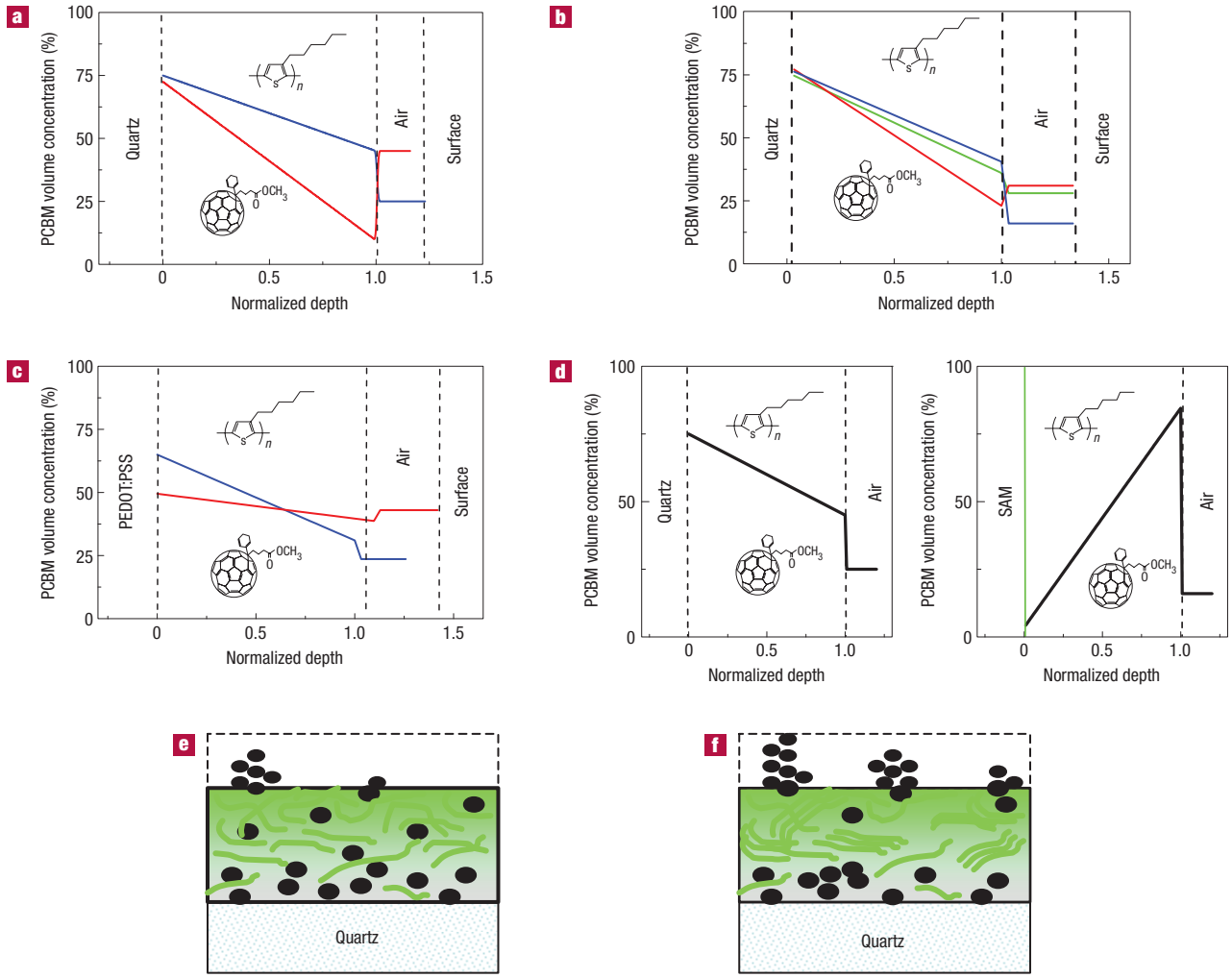

Figure 3 Vertical composition profiles in P3HT:PCBM films as deduced using ellipsometry. a–d, PCBM concentration profiles obtained from analysis of ellipsometric data for P3HT:PCBM blend films: **a**, spin coated on fused silica before (blue) and after (red) thermal annealing; **b**, spin coated on fused silica for 60 s at 5,000 r.p.m. (blue), 3,000 r.p.m. (green) and 700 r.p.m. (red) (the blend films here were typically ~50 nm thick); **c**, spin coated on PEDOT:PSS-coated fused silica before (blue) and after (red) vapour annealing; **d**, spin coated on fused silica (left) and on a Si wafer (with native oxide) precoated with a hydrophobic self-assembled hexamethyldisilazane monolayer. **e**,**f**, Schematic representations of the model used to fit the ellipsometry data, showing typical PCBM distributions before (**e**) and after (**f**) vapour or thermal annealing. Note that PCBM crystals in real samples are often much larger than illustrated here.

increases. The similar effects of the two processing regimes on composition profile, as well as on P3HT crystallinity as observed in Fig. 1a, may well explain why optimized solar cells fabricated using thermal annealing and slow drying result in comparable PCE values[7,8]. A third treatment, vapour annealing, where an untreated film is exposed to a solvent-saturated atmosphere, results in similar morphology changes (see Supplementary Information, Fig. S2) and a correspondingly improved EQE (Fig. 1b). The similarity in the changes for all three protocols suggests that the enhanced molecular mobility that they afford relative to fast spin coating enables the molecules to reach a more thermodynamically favourable morphology. Moreover, this morphology seems to be qualitatively independent of the specific fabrication protocol. We should, however, note that the magnitudes of the changes for each of the three protocols depend subtly on parameters such as solution concentration, final film thickness and duration of treatment; here we show only representative examples. The direction of vertical phase segregation observed here for blend films on fused silica is opposite to that which would be required for improved solar cell performance in typical device architectures with a bottom anode: we explain this apparent contradiction below, noting that the directionality can be controlled by specific surface interactions.

Real-time *in situ* ellipsometry can further elucidate the mechanism by which these treatments affect the morphology. The observation of a sharp change in P3HT oscillator strength as a reference (untreated) sample is heated past 100 °C indicates the onset of P3HT crystallization in the blend (Fig. 4e). From this point onwards, the film oscillator strength increases as a result of closer packing of the polymer chains[37] whilst the ellipsometrically determined film thickness decreases (Fig. 4e). Analysis of VASE measurements carried out at different temperatures further indicates that the diffusion of PCBM becomes faster as the polymer starts to crystallize. This is also observed for vapour-annealed films. By measuring at wavelengths characteristic of PCBM (275 nm) or

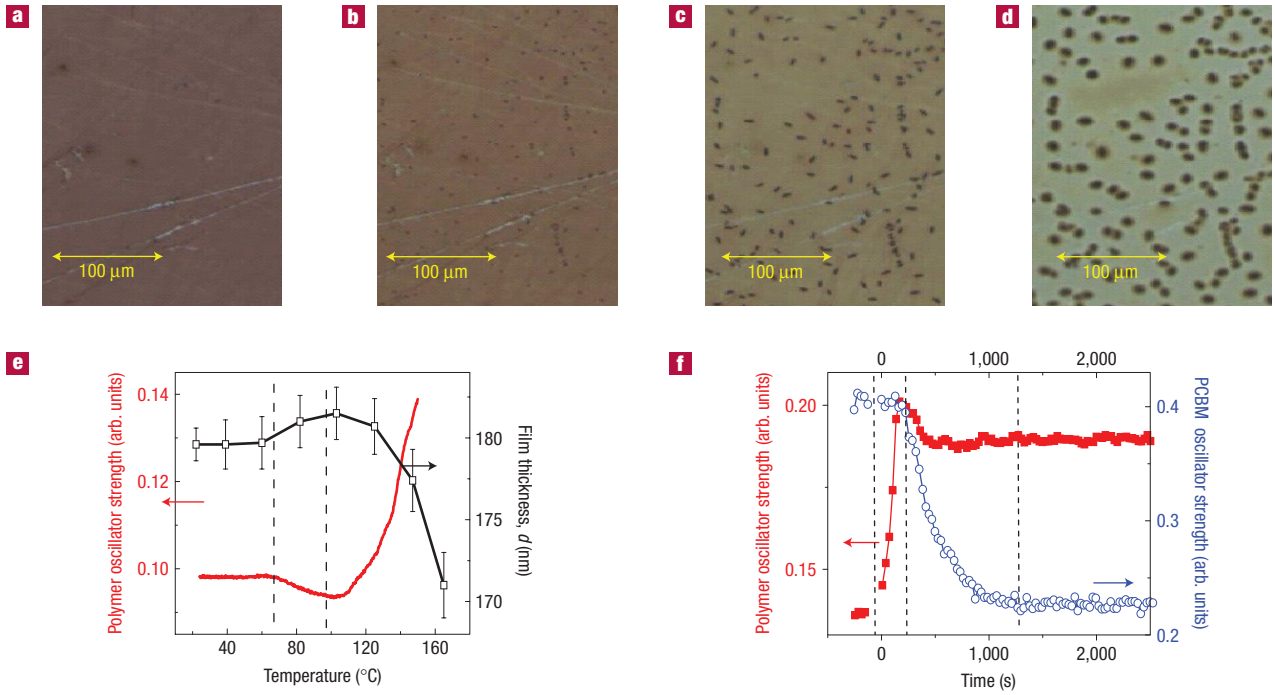

Figure 4 Real-time evolution of P3HT:PCBM blend morphology. a–d, Optical micrographs of the surface of a P3HT:PCBM blend film spin coated on quartz, taken during a continuous heating cycle at a rate of 10 °C min^{-1}. The images in **a–d** correspond to temperatures of 70, 160, 184 and 250 °C, respectively. The changes in colour visible during this treatment may correspond to P3HT crystallization (which would occur on going from 70 to 160 °C), followed by melting (on going from 184 to 250 °C), as well as to PCBM depletion; several scratches (due to sample transportation) and inhomogeneities (introduced during the spin coating) can be seen in **a**. **e**, *In situ* ellipsometry measurements for a 1:1 P3HT:PCBM blend heated at 1 °C min^{-1}. The red line represents a continuous scan up to 160 °C (the limit of our apparatus), with increasing temperature, of the ellipsometric angle tan Ψ at 525 nm, which is proportional to the polymer oscillator strength at this resonant wavelength. The open squares are the film thicknesses deduced from spectroscopic ellipsometry scans at fixed temperatures (the solid line is a guide to the eye); the oscillator strength is proportional to the inverse of thickness, indicating that in this case the oscillator strength (and tan Ψ) is a measure of density; the two dashed lines delineate a softening temperature around 70 °C and the onset of P3HT crystallization (~100 °C). Error bars in the film thickness are the corresponding fitting uncertainties (derived using the Levenger–Marquardt algorithm) obtained during the analysis of the spectroscopic ellipsometry data at each temperature. **f**, Time evolution of tan Ψ at 525 nm (red) and 275 nm (blue) of a blend film exposed to a saturated chlorobenzene atmosphere (exposure starts at time = 0). Tan Ψ at 525 (275) nm is proportional to the P3HT (PCBM) oscillator strength (and hence to the density) in the plane of the substrate. The first vertical dashed line indicates when the solvent vapour was introduced. Between the first and second dashed lines, the rise in oscillator strength indicates the crystallization of P3HT (ref. 42). This is followed by the diffusion of PCBM (seen here as a decrease in the in-plane density) and possibly a crystal reorganization of the P3HT crystals (a small decrease in the polymer oscillator strength). The dashed line at around 1,200 s corresponds to the onset of film stabilization.

P3HT (550 nm) absorption (compare Fig. 1a and Supplementary Information, Fig. S1a), we can selectively investigate the effect of a particular treatment on each component in a blend film. Figure 4f shows the variations in PCBM and P3HT average oscillator strength (density) in a blend film as a function of vapour annealing time. It can be seen that P3HT chains start to crystallize as soon as the vapour is introduced, as reflected by the rapid increase in oscillator strength (densification). Only once the polymer has crystallized does the PCBM start to diffuse to neighbouring nucleation sites, resulting in a decreasing oscillator strength (density) in those areas from which it diffuses. The same behaviour is observed on thermal annealing, consistent with the earlier conclusion that the two treatments have equivalent effects on the morphology of the blend film. These *in situ* experiments show an onset in the diffusion of PCBM molecules that is apparently linked to the polymer crystallization process, a proposal that would be consistent with the thermally induced changes reported for P3HT:semicrystalline-PS blends[29]. A possible interpretation is that PCBM diffusion occurs more readily through low-polymer-density pathways that open up between P3HT crystallites.

The different effects on device EQE of thermal annealing before and after deposition of the top contact (Fig. 1b and ref. 38) suggest that boundary conditions may significantly influence the final morphology. In a previous study of poly(2-methoxy-5-(3,7-dimethyloctyloxy)-1,4-phenylenevinylene):PCBM blend films it was also shown that the degree of fullerene molecule diffusion, quantified by the resultant size of PCBM crystallites formed on thermal annealing, is greater for singly bounded (sitting on a substrate) than doubly bounded (sandwiched between a substrate and a top LiF/Al contact) films, and greatest of all for unbounded (free-standing) films[23]. This can be understood in terms of the enhanced free volume present at the unbounded (air) surface(s)[39–42]. Here, we observe that the addition of an ultrathin (circa 8 nm) optically semitransparent evaporated Al layer on top of a blend film does not substantially modify the vertical segregation profile (see Supplementary Information, Fig. S3). Our ellipsometry results suggest that thicker (and optically opaque) Al layers would be needed to prevent the formation of large surface-segregated PCBM clusters on postevaporation annealing (see the Supplementary Information), in support of the free-volume hypothesis.

As already noted, specific interactions between the organic materials and the substrate should also have a strong effect on morphology[42,43]. Figure 3c shows the concentration

profile of a P3HT:PCBM film deposited on poly(3,4-ethylenedioxythiophene):poly(styrenesulfonate) (PEDOT:PSS), a conducting polymer commonly used to coat ITO anodes in polymer devices. Untreated P3HT:PCBM blend films spin coated on PEDOT:PSS present a qualitatively similar negative (that is, unfavourable for electrode selectivity) concentration profile to the films spin coated directly on fused silica, but with a somewhat less negative gradient. We note that this behaviour was confirmed in measurements on more than 10 samples of different thicknesses. It thus seems that the presence of the conducting polymer may slightly inhibit the segregation of the two components in the vertical direction, probably due to the difference in surface energy. On vapour (Fig. 3c) or thermal (not shown) annealing, the vertical profile is changed such that the P3HT concentration at the PEDOT:PSS anode is increased, in sharp contrast to the case of films spin coated on fused silica, where the P3HT concentration at the anode is further depleted on annealing. Thus, in the case of PEDOT:PSS substrates, the vertical phase segregation becomes more positive (better for electrode selectivity) on annealing, and as such is expected to benefit solar cell performance.

To further illustrate the effect of the blend–substrate interface, we can coat the substrate with molecular self-assembled monolayers with different properties. Figure 3d compares the case of an untreated reference blend film spin coated on fused silica (left graph) and on a silicon/SiO_2 substrate covered by a hydrophobic self-assembled monolayer, namely hexamethyldisilazane. When the surface energy of the substrate is modified in this way the compositional gradient changes sign, with P3HT now preferentially found close to the substrate and PCBM displaced towards the free (air) surface. These results clearly demonstrate that the direction of the vertical segregation can be controlled by the surface energy of the substrate, with the degree of segregation further controlled by annealing or other treatments that modify molecular mobility.

Vertical segregation of donor towards anode and acceptor towards cathode in organic photovoltaic devices represents a compromise between a planar and a distributed heterojunction, and potentially offers the advantages of both configurations: efficient exciton dissociation as a result of the intimate intermixing of components, and efficient charge transport and enhanced electrode selectivity as a result of the segregation[30]. We note again that the preferred segregation direction for a typical photovoltaic device (with the anode, for example ITO/PEDOT:PSS, on the substrate) is that illustrated by the blend spin coated onto the hydrophobic self-assembled monolayer, where the donor (P3HT) is concentrated close to the substrate, and the acceptor (PCBM) next to the top surface, onto which the cathode (for example Al) would be deposited. This distribution of components is expected to enhance the selectivity of the contacts towards one type of charge carrier and so reduce charge leakage. Even in the case of blends deposited on PEDOT:PSS-coated anodes, vapour and thermal annealing lead to a more favourable composition profile (Fig. 3c) than the untreated case. This improvement in electrode selectivity with annealing will help to increase the shunt resistance (and so the fill factor) of the device under illumination[7,9], and consequently the overall PCE of the solar cell.

Although our dynamic studies suggest that the effects of P3HT crystallization and PCBM diffusion are strongly correlated, it is possible to look at them semi-independently in given scenarios. Table 1 shows the effect of thermal (140 °C) annealing time on quartz/PEDOT:PSS/blend films and on full devices. P3HT crystallization, as deduced from the optical absorption around 520 nm (ref. 16) (Table 1 and Supplementary Information, Fig. S4a), saturates after around 5 min of annealing. PCBM diffusion, as quantified by the changes in the concentration profile, also progresses over this period of time. However, the gradient continues to increase (become more positive) on further annealing. The increase in device PCE relative to the untreated devices during the first (5 min) annealing stage is attributed to both P3HT crystallization and PCBM diffusion. The further increase in PCE from 3.64% to 3.92%, is, however, attributed only to PCBM diffusion because P3HT crystallization is complete. (For further device data see the Supplementary Information.) This example confirms that both crystallization and diffusion effects must be included in any complete description of the morphology evolution of polymer:fullerene films and its effect on device performance.

Table 1 Optical density (OD) and slope of the PCBM vertical profile for P3HT:PCBM (1:1) blend films deposited on PEDOT:PSS, and power conversion efficiency (PCE) for solar cells as a function of annealing time (at 140 °C).

Annealing time (min)	OD(520 nm) (arb. units)	Slope (on PEDOT) (%)	PCE (%)
0	0.709	−25	1.13
5	0.879	−6.8	3.64
30	0.879	−5.9	3.92

We would note, further, that vertical segregation can also have a strong impact on the performance of other types of device based on polymers, specifically organic field-effect transistors, where the composition of a thin layer next to the substrate dominates performance[29]. For the P3HT:PCBM system, our results suggest (and this is supported by preliminary studies) that the ambipolar character of the blend can be tuned to give unipolar characteristics (of either sign) by an appropriate choice of substrate and annealing conditions.

METHODS

Regioregular P3HT was synthesized by Merck Chemicals and used as received. The typical weight- and number-average molecular weights, polydispersity index, melting point and regioregularity were 2.11×10^4, 1.16×10^4, 1.82, 222 °C and ~95.4%, respectively. PCBM was used as received from the University of Groningen, The Netherlands[44]. Pristine P3HT and PCBM solutions were prepared using chlorobenzene (20 mg ml^{-1}). Blend solutions (P3HT:PCBM = 1:1 by weight) were also prepared using chlorobenzene (30 mg ml^{-1}). The solutions were stirred overnight to promote complete dissolution.

Spectrosil B fused-silica substrates (Kaypul Optics Limited, UK) were cleaned in sequence with acetone (15 min) and isopropanol (15 min) using an ultrasonic bath, and then dried using a nitrogen gun. The pristine material and blend films were then prepared by spin coating their respective solutions at a variety of spin speeds/times on top of cleaned substrates. Some samples were also prepared with a PEDOT:PSS (Baytron P standard grade, HC Stark) layer spin coated (3,000 r.p.m. for 1 min) from aqueous solution on to the cleaned Spectrosil substrates and annealed at 200 °C for 30 min. PEDOT:PSS films (without a blend film on top) were also measured using VASE to provide reference data for the analysis of the PEDOT:PSS–blend film samples. We used four fabrication protocols: (1) fast spin coating (spin speeds greater than 2,000 r.p.m., for a period of 60 s to give 'untreated' films), (2) slow drying (either spin speed slower than 1,000 r.p.m. for 60 s or spin coated at 2,000 r.p.m. for times shorter than 10 s and left to dry), (3) thermally annealed (after fast spin coating) in a glove box filled with nitrogen and (4) solvent annealed by exposure to a solvent- (chlorobenzene-) vapour-saturated atmosphere at room temperature. In addition, some films were half covered with an ultrathin (circa 8 nm) Al layer deposited *in vacuo* (4×10^{-6} mbar) by thermal evaporation.

Absorption spectra were measured at normal incidence using a ultraviolet–visible spectrophotometer (V-560, Jasco). VASE was carried out using a SOPRA rotating polarizer (GESP 5) ellipsometer. Three incidence angles were recorded (close to the Brewster angle of each sample), with the wavelength scanned from 250 to 850 nm (5 nm steps). We note that the morphology evolution on fused silica substrates is qualitatively similar to that on device substrates. Hence, for simplicity of analysis (reducing the number of optically distinct layers that need to be incorporated in the model), and thus to give confidence

in the assessment procedure we develop, most of the VASE measurements have been carried out for blend films on fused silica substrates. We have first characterized the optical constants of films comprising purely PCBM and purely P3HT spin coated on fused silica substrates (see Supplementary Information, Fig. S1a) using the standard critical point model of the dielectric function[45]. We note that pristine films were measured before and after annealing: the effect on the optical constants was minor[13]. Then, the data for the blend films on fused silica substrates were fitted using four different models for the blend composition profile, namely (1) a homogeneous distribution of the two components, (2) a vertically graded composition, (3) a bilayer comprising a homogeneous distribution layer capped by a mixed PCBM–air layer and (4) a bilayer comprising a vertically graded layer capped by a mixed PCBM–air layer (see Supplementary Information Fig. S1c–f for further details).

Confocal Raman microscopy measurements were made with a ultraviolet–visible Jobin–Yvon LabRam confocal microscope system equipped with notch filters and a nitrogen-cooled ultraviolet-enhanced CCD (charge-coupled device) detector. Ultraviolet excitation (~0.5 mW, 325 nm, He–Cd laser light) was used and the scattered Raman signal was collected with a ×40 ultraviolet objective (~1 mm working distance). Measurements were made at five to ten locations on each sample in order to ensure the representative and consistent nature of the reported signals. We specifically used selective wavelength Raman spectroscopy, where we excited at the resonant wavelength (lying around the maximum of absorption) of each material. As shown in Fig. 2e, by exciting at 325 nm we obtain mainly a signal corresponding to the PCBM molecules in the blend. If the excitation wavelength is around 550 nm, then we can monitor P3HT chains.

The surface morphology of the blend films was examined using a multimode scanning probe microscope system (tapping mode AFM, Digital Instrument, USA).

Photovoltaic devices were also prepared using the four treatment protocols described above. The blends were in this case spin coated on top of an ITO/PEDOT:PSS-coated glass substrate, and thermally evaporated Al contacts were deposited on top. We thermally annealed some of these devices both before and after the top contact was evaporated. The device characteristics were measured in the standard way, as for instance previously reported in refs 7,9.

Received 17 April 2007; accepted 13 December 2007; published 20 January 2008.

References

1. Halls, J. J. M. *et al.* Efficient photodiodes from interpenetrating networks. *Nature* **376**, 498–500 (1995).
2. Yu, G., Gao, J., Hummelen, J. C., Wudl, F. & Heeger, A. J. Polymer photovoltaic cells: Enhanced efficiencies via a network of internal donor–acceptor heterojunctions. *Science* **270**, 1789–1791 (1995).
3. Hoppe, H. & Sariciftci, N. S. Morphology of polymer/fullerene bulk heterojunction solar cells. *J. Mater. Chem.* **16**, 45–61 (2006).
4. Shaheen, S. E. *et al.* 2.5% efficient organic plastic solar cells. *Appl. Phys. Lett.* **78**, 841–843 (2001).
5. Ma, W., Yang, C., Gong, X., Lee, K. & Heeger, A. J. Thermally stable, efficient polymer solar cells with nanoscale control of the interpenetrating network morphology. *Adv. Funct. Mater.* **15**, 1617–1622 (2005).
6. Reyes-Reyes, M., Kim, K. & Carroll, D. L. High-efficiency photovoltaic devices based on annealed poly(3-hexylthiophene and 1-(3-methoxycarbonyl)-propyl-1-phenyl-(6,6) C_{61} blends. *Appl. Phys. Lett.* **87**, 083506 (2005).
7. Kim, Y. *et al.* A strong regioregularity effect in self-organizing conjugated polymer films and high-efficiency polythiophene:fullerene solar cells. *Nature Mater.* **5**, 197–203 (2006).
8. Li, G. *et al.* High-efficiency solution processable polymer photovoltaic cells by self-organization of polymer blends. *Nature Mater.* **4**, 864–868 (2005).
9. Kim, Y. *et al.* Device annealing effect in organic solar cells with blends of regioregular poly(3-hexylthiophene) and soluble fullerene. *Appl. Phys. Lett.* **86**, 063502 (2005).
10. Vanlaeke, P. *et al.* Polythiophene based bulk heterojunction solar cells: Morphology and its implications. *Thin Solid Films* **511–512**, 358–361 (2006).
11. Mihailetchi, V. D. *et al.* Origin of the enhanced performance in poly(3-hexylthiophene):[6,6]-phenyl C_{61}-butyric acid methyl ester solar cells upon slow drying of the active layer. *Appl. Phys. Lett.* **89**, 012107 (2006).
12. Kim, K., Liu, J. & Carroll, D. L. Thermal diffusion processes in bulk heterojunction formation from poly-3-hexylthiophene/C_{60} single heterojunction photovoltaics. *Appl. Phys. Lett.* **88**, 181911 (2006).
13. Chirvase, D., Parisi, J., Hummelen, J. C. & Dyakonov, V. Influence of nanomorphology on the photovoltaic action of polymer–fullerene composites. *Nanotechnology* **15**, 1317–1323 (2004).
14. Zhao, Y., Xie, Z., Qu, Y., Geng, Y. & Wang, L. Solvent-vapor treatment induced performance enhancement of poly(3-hexylthiophene):methanofullerene bulk-heterojunction photovoltaic cells. *Appl. Phys. Lett.* **90**, 043504 (2007).
15. Osterbacka, R., An, C. P., Jiang, X. M. & Vardeny, Z. V. Two-dimensional electronic excitations in self-assembled conjugated polymer nanocrystals. *Science* **287**, 839–842 (2000).
16. Zhokhavets, V., Erb, T., Gobsch, G., Al-Ibrahim, M. & Ambacher, O. Relation between absorption and crystallinity of poly(3-hexylthiophene)/fullerene films for plastic solar cells. *Chem. Phys. Lett.* **418**, 347–350 (2006).
17. Vanlaeke, P. *et al.* P3HT/PCBM bulk heterojunction solar cells: Relation between morphology and electro-optical characteristics. *Sol. Energy Mater. Sol. Cells* **90**, 2150–2158 (2006).
18. Klimov, E., Li, W., Yang, X., Hoffmann, G. G. & Loos, J. Scanning near-field and confocal Raman microscopic investigation of P3HT-PCBM systems for solar cell applications. *Macromolecules* **39**, 4493–4496 (2006).
19. Yang, X. *et al.* Nanoscale morphology of high-performance polymer solar cell. *Nano Lett.* **5**, 579–583 (2005).
20. Zhokhavets, V., Erb, T., Hoppe, H., Gobsch, G. & Sariciftci, N. S. Effect of annealing of poly(3-hexylthiophene)/fullerene bulk heterojunction composites on structural and optical properties. *Thin Solid Films* **496**, 679–682 (2006).
21. Savenije, T. J., Kroeze, J. E., Yang, X. & Loos, J. The effect of thermal treatment on the morphology and change carrier dynamics in a polythiophene-fullerene bulk heterojunction. *Adv. Funct. Mater.* **15**, 1260–1266 (2005).
22. Swinnen, A. *et al.* Tuning the dimensions of C_{60}-based needlelike crystals in blended thin films. *Adv. Funct. Mater.* **16**, 760–765 (2006).
23. Yang, X., Alexeev, A., Michels, A. J. & Loos, J. Effect of spatial confinement on the morphology evolution of thin poly(p-phenylenevinylene)/methanofullerene composite films. *Macromolecules* **38**, 42890–4295 (2005).
24. Tompkins, H. G. & Irene, E. A. (eds) *Handbook of Ellipsometry* (William Andrew Publishing, Norwich, New York, 2005).
25. Fried, M. *et al.* Dose-dependence of ion implantation-caused damage in silicon measured by ellipsometry and backscattering spectrometry. *Thin Solid Films* **455**, 404–409 (2004).
26. Zaumseil, P., Krüger, D., Kurps, R., Fursenko, O. & Formanek, P. Precise measurement of Ge depth profiles in SiGe HBT's—a comparison of different methods. *Solid State Phenom.* **95–96**, 473–482 (2004).
27. Reyes-Reyes, M. *et al.* Meso-structure formation for enhanced organic photovoltaic cells. *Org. Lett.* **7**, 5749–5752 (2005).
28. Waldauf, C. *et al.* Highly efficient inverted organic photovoltaics using solution based titanium oxide as electron selective contact. *Appl. Phys. Lett.* **89**, 233517 (2006).
29. Goffri, S. *et al.* Multicomponent semiconducting polymer systems with low crystallization-induced percolation threshold. *Nature Mater.* **5**, 950–956 (2006).
30. Arias, A. C. *et al.* Vertically segregated polymer-blend photovoltaic thin-film structures through surface-mediated solution processing. *Appl. Phys. Lett.* **80**, 1694–1697 (2002).
31. Björnström, C. M. *et al.* Multilayer formation in spin-coated thin films of low-bandgap polyfluorene:PCBM blends. *J. Phys. Condens. Matter* **17**, L529–L534 (2005).
32. Björnström, C. M. *et al.* Vertical phase separation in spin-coated films of a low bandgap polyfluorene/PCBM blend—effects of specific substrate interaction. *Appl. Surf. Sci.* **253**, 3906–3912 (2007).
33. Heriot, S. Y. & Jones, R. A. L. An interfacial instability in a transient wetting layer leads to lateral phase separation in thin spin-cast polymer-blend films. *Nature Mater.* **4**, 782–786 (2005).
34. Snaith, H. J., Greenham, N. C. & Friend, R. H. The origin of collected charge and open-circuit voltage in blended polyfluorene photovoltaic devices. *Adv. Mater.* **16**, 1640–1645 (2004).
35. Xue, J., Rand, B. P., Uchida, S. & Forrest, S. R. Mixed donor–acceptor molecular heterojunctions for photovoltaic applications. II. Devices performance. *J. Appl. Phys.* **98**, 124903 (2005).
36. Heutz, S., Sullivan, P., Sanderson, B. M., Schultes, S. M. & Jones, T. S. Influence of molecular architecture and intermixing on the photovoltaic, morphological and spectroscopic properties of CuPc–C60 heterojunctions. *Sol. Energy Mater. Sol. Cells* **83**, 229–245 (2004).
37. Sims, M. *et al.* On the use of optical probes to monitor the thermal transitions in spin-coated poly(9,9-dioctylfluorene) films. *J. Phys. Condens. Matter* **17**, 1–12 (2005).
38. Kim, H., So, W.-W. & Moon, S.-J. Effect of thermal annealing on the performance of P3HT/PCBM polymer photovoltaic cells. *J. Kor. Phys. Soc.* **48**, 441–445 (2006).
39. Si, L., Massa, M. V., Dalnoki-Veress, K., Brown, H. R. & Jones, R. A. L. Chain entanglement in thin freestanding polymer films. *Phys. Rev. Lett.* **94**, 127801 (2005).
40. Ellison, C. J. & Torkelson, J. M. The distribution of glass-transition temperatures in nanoscopically confined glass formers. *Nature Mater.* **2**, 695–700 (2003).
41. Sharp, J. S. & Forrest, J. A. Free surfaces cause reductions in the glass transition temperature of thin polystyrene films. *Phys. Rev. Lett.* **91**, 235701 (2003).
42. Campoy-Quiles, M., Sims, M., Etchegoin, P. G. & Bradley, D. D. C. Thickness-dependent thermal transition temperatures in thin conjugated polymer films. *Macromolecules* **39**, 7673–7680 (2006).
43. van Zanten, J. H., Wallace, W. E. & Wu, W.-L. Effect of strongly favourable substrate interaction on the thermal properties of ultrathin polymer films. *Phys. Rev. E* **53**, R2053–R2056 (1996).
44. Hummelen, J. C. *et al.* Preparation and characterization of fulleroid and methanofullerene derivatives. *J. Org. Chem.* **60**, 532–538 (1995).
45. Campoy-Quiles, M. *et al.* Ellipsometric characterization of the optical constants of polyfluorene gain media. *Adv. Funct. Mater.* **15**, 925–933 (2005).

Acknowledgements

The authors thank the UK Engineering and Physical Sciences Research Council (project no. EP4/C5403361) and BP Solar (OSCER project) for financial support. We also thank I. McCulloch, M. Heeney and M. Giles, from Merck Chemicals, for supplying the P3HT polymer. M.C.-Q. thanks S. Choulis, S. Sidat and S. Sohel for useful discussions at the early stages of these investigations, J. Dane for help with the evaporation mask designs and Rod Bottom and Phil Williams (Mettler Toledo Ltd) for their help with the real-time microscopy measurements.
Correspondence and requests for materials should be addressed to M.C.-Q., D.D.C.B. or J.N.
Supplementary Information accompanies this paper on www.nature.com/naturematerials.